Supporting information

Experimental

Materials:

All the materials were purchased from commercial suppliers and used without further purification unless otherwise noted.

Synthesis of PEEKK

The synthesis of phenyl poly(ether ether ketone ketone) was the same as that descried in Ref. S1, and the synthesis route is shown in Scheme S1.

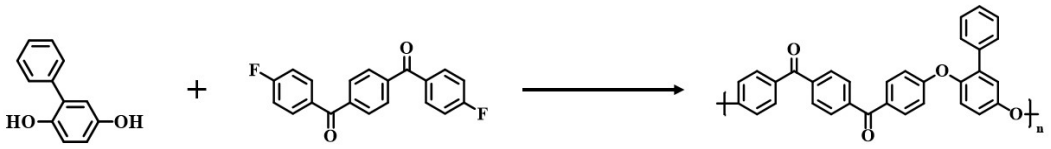

Scheme S1. Synthetic route of Ph-PEEKK.

Synthesis of PAF-6-Li

The synthesis of PAF-6 was the same with that in Ref. S2 and S3. The synthesis steps are shown in Scheme S2. PAF-6 was prepared in the A3 (cyanuric chloride) + B2 (piperazine) reaction system via a one-step polymerization. The polymerization was first carried out in an ice-bath for 4 h and the temperature was slowly raised to 90 °C. The precipitate was collected and washed with THF and H_2O repeatedly.

The prepared PAF-6 (100 mg) was uniformly dispersed in dichloromethane (10 mL) in an ice-water bath, and chlorosulfonic acid (1.0 mL, 15 mmol) was added, and stirred at room temperature for three days. Then, the mixture was poured into ice water, the solid was collected, and the material was washed with deionized water several times to obtain PAF-6-SO_3H.

PAF-6-SO_3H was dispersed uniformly in dichloromethane and deionized water (10 mL/10 mL), and LiOH (1.0 g) was added and stirred at room temperature for three days for lithiation. Then, the mixture was poured into deionized water, the solid was collected, and washed with deionized water several times to obtain the product, named as PAF-6-SO_3Li [4]. The obtained PAF-6-SO_3Li was injected with LiTFSI by vacuum infusion. After drying, the product was obtained and named as PAF-6-Li. The preparation of PAF-6-Li is shown in Scheme S2.

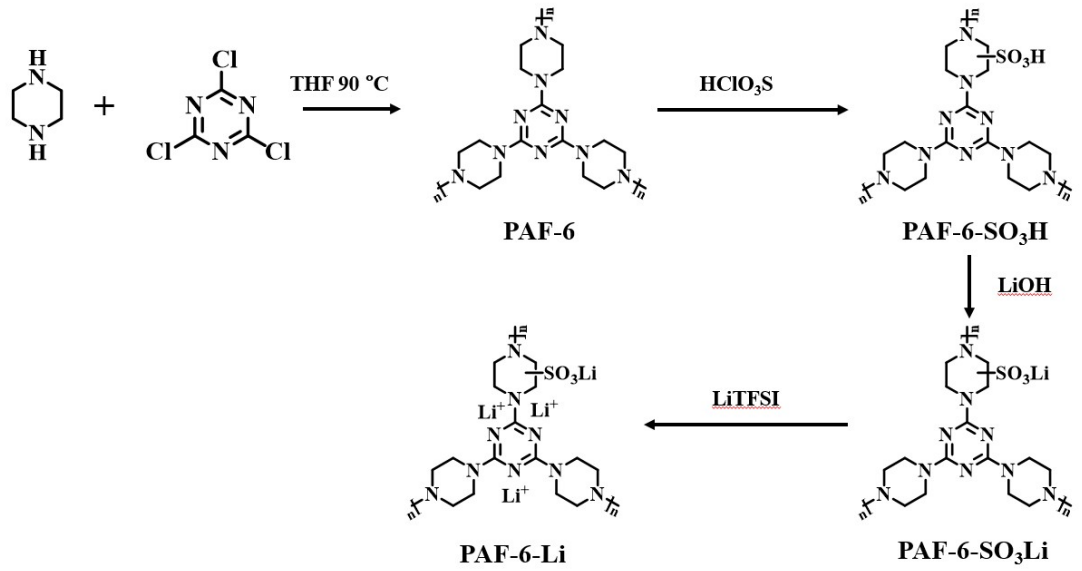

Scheme S2. Preparation of PAF-6-Li.

Preparation of nanocellulose（NCC）

20 g micron cellulose (MCC) was added into 300 mL sulfuric acid (mass fraction 64%), stirred at 45 °C for 3 h, then poured into a large amount of deionized water to form a suspension. The suspension was centrifuged for 10 min several times (10000 rpm). The acid in the suspension was removed by dialysis. The white NCC was obtained after freeze-drying.

Preparation of Janus membranes

Firstly, PEEKK was dissolved in a solution of sulfuric acid and methyl sulfonic acid with a mass ratio of sulfuric acid/methyl sulfonic acid of 1:10 to prepare a 7% casting solution at room temperature. Then, NCC with a mass ratio of 1% to PEEKK was added. Furthermore, PAF-6-Li with a mass content of 5% to PEEKK was added to get the phase conversion solution.

The Janus membranes were prepared by the phase inversion method. The phase conversion solutions were scrapped on one side of the Celgard 2500 separator (PE), and then transferred to methanol/water solution ($V_{methanol}$: V_{water} = 1 : 4). The thickness was set as 15 μm. The phase inversion process was about 0.5 h at room temperature. Then, the modified separator was taken out, washed with deionized water, and dried in vacuum at 70 °C to obtain Janus membranes (PCP@PE). Other samples were prepared with the same method. The composite membrane prepared with only PEEKK solution through the phase conversion solution was named as P@PE, and the Janus composite

membrane prepared with the solution of PEEKK and NCC through the phase conversion solution was named as PC@PE.

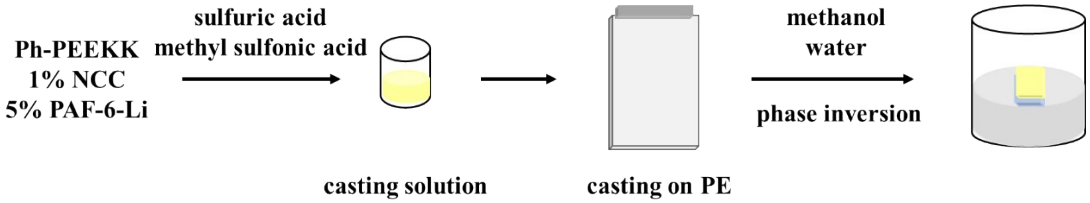

Scheme S3. Preparation route of Janus membranes PCP@PE.

Characterization methods

FT-IR spectra were obtained on the Nicolet IS50 Fourier Transform Infrared spectrometer. ^{1}H NMR spectra were performed on a Bruker Advance NEO 500 NMR spectrometer. The surface area and pore size distribution were obtained with the Micromeritics ASAP 2020M Accelerated Surface Area and Porosimetry System. Scanning Electron Microscopy (SEM) was performed with a Hitachi SU8010 Field-emission Scanning Electron Microscope. Transmission Electron Microscopy (TEM) was performed with a JEM-2100 PLUS Transmission Electron Microscope. Mechanical properties were obtained with a Shimadzu AG-I 1kN Electronic Universal material testing machine. Thermal stability testing of the samples were performed on TAQ50 Thermal Gravimetric Analyzer (TGA) Instrument at a heating rate of 10 °C min^{-1} from 30 to 700 °C under N_2 atmosphere. The gas flow rate was 60 mL min^{-1}.

Electrochemical measurements

The mass ratio S: Ketjen Black: Polyvinylidene Fluoride (PVDF) =6:3:1 was mixed in NMP and coated on aluminum foil. After vacuum drying, it was stamped into wafers as the cathode. Lithium was used as the anode, and the modified composite separator was used as the separator. 20 μL of electrolyte (1 mol L^{-1} of LiTFSI in DOL/DME (1:1, volume ratio) solution with 0.2% $LiNO_3$) was added in to assemble a cr2025 button cell. All the above operations were carried out in the glove box. The active material content was approximately 2 mg cm^{-2}. Neware was selected as the test system.

The stainless steel sheet (SS)/separator/SS battery was assembled and used to test the ionic conductivity of the separator with the electrochemical workstation (Autolab PGSTAT302N). The test frequency range was 1 MHz-50 MHz, and the disturbance voltage was 10 mV.

The lithium ion conductivity of the separator is calculated based on the following equation:

$\sigma = d/(A \cdot Rb)$

σ represents the ionic conductivity, d represents the thickness of the separator, A represents the area of the stainless steel electrode, and R_b represents the impedance. Among them, the EIS test can obtain the impedance R_b, the d of the diaphragm is measured with a spiral micrometer, the radius of the stainless steel electrode is measured with a ruler, and the A of the stainless steel electrode is calculated by using the area formula of the circle.

The Li/separator/Li battery was assembled and used to calculate the diffusion coefficient of lithium ions with the electrochemical workstation (Autolab PGSTAT302N). The symmetrical battery was polarized at disturbance voltage of 10 mV (ΔV) at 25 °C. t_{Li+} was calculated according to the following formula [5]:

$$t_{Li}^{+} = I_{ss}(\Delta V - I_0 R_0) / I_0(\Delta V - I_{ss} R_{ss}) \quad (1)$$

Among them, I_0 and I_{ss} was the current before and after polarization respectively; R_0 and R_{ss} was the voltage before and after polarization respectively.

Cyclic voltammetry (CV) and electrochemical impedance (EIS) were tested with electrochemical workstation (Autolab PGSTAT302N). The voltage range was 1.7-2.8 V and the sweep speed was 0.1 mV s^{-1} in CV measurement. The frequency range was 0.1-105 Hz, and the disturbance voltage was 10 mV in the AC impedance.

Mechanical property measurements

The mechanical performance test was measured at room temperature by AG-I 1kN tensile testing machine. The separator sample was cut into the size of 45×5 mm, with the tensile rate of 5 mm/min, and 5 parallel samples were tested in each group. The average values obtained were the final result.

Thermal analysis

The thermal stability of the separator was characterized by observing the dimensional changes of the separator in different temperature. The separator samples were cut into discs, placed in a 180 °C oven, maintained stable for 30 minutes, and then taken out to observe the dimensional changes of the separator.

Porosity analysis

The separator was cut into the size of 2×2 cm, measured the thickness, calculated the volume V, and weighed the mass W_a of the dry porous separator, and then soak it in n-butanol for 2 h, and wiped off the excess n-butanol with filter paper. Weighed the

mass W_b of the wet porous separator and calculated the porosity according to the following formula:

$$P = (W_b - W_a) / \rho V \times 100 \qquad (2)$$

Among them, W_a and W_b was the mass of separator before and after absorbing n-butanol respectively. ρ was the density of n-butanol, and V was the volume of the separator.

Loading rate analysis

The separator was cut into the size of 2×2 cm,, accurately weighed mass W_a, then immersed the separator in the electrolyte, and after soaking for 2 hours, took out the sample and weighed its mass W_b. Calculated liquid absorption rate according to the following formula :

$$W\% = (W_a - W_b) / W_b \times 100\% \qquad (3)$$

Among them, W_a and W_b was the mass of separator before and after absorbing electrolyte respectively.

Results and discussion

^{1}H NMR of sulfonated phenyl poly(ether ether ketone ketone) (SPEEKK)

The ^{1}H NMR of SPEEKK is shown in Figure S1. The result illustrated that the expected structure is obtained. The degree of sulfonation was determined to be 0.89 [1].

^{1}H NMR (400 MHz, DMSO) δ 8.00-7.61 (m, 9H), 7.59 (s, 2H), 7.51 (d, J = 7.8 Hz, 3H), 7.40 -7.14 (m, 6H), 7.07 (d, J = 8.3 Hz, 3H).

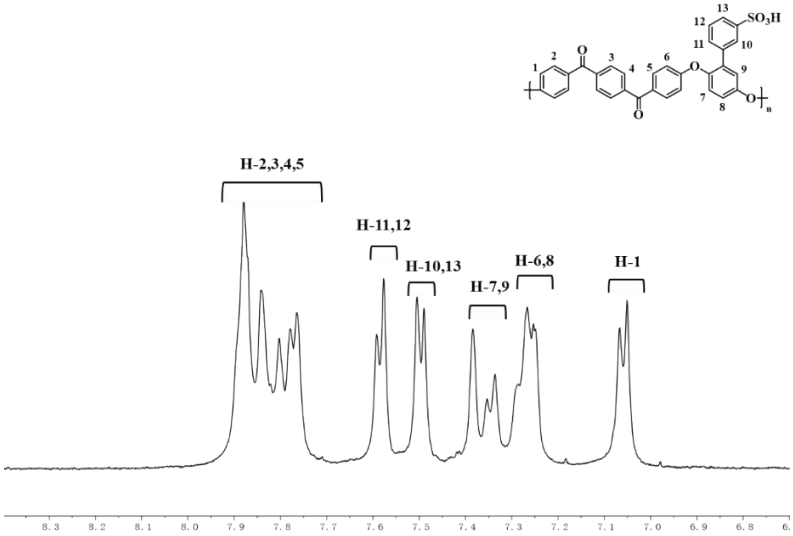

Figure S1. ^{1}H NMR of SPEEKK.

Thermal stability

The TGA curves of PAF-6 and PAF-6-Li are shown in Figure S2(a). PAF-6 began to degrade at 400 °C, which corresponds to the collapse of the structure [7]. The weight loss of PAF-6-Li began at about 200 °C should be caused by the loss of the crystal water in LiTFSI [8]. And the thermal decomposition at 350 °C was caused by the decomposition of LiTFSI [9]. The TGA curve of the composite separators is shown in Figure S2(b). PC@PE started to degrade at 200 °C, which corresponded to the degradation of NCC [10]. PCP@PE also began to degrade at about 200 °C, and the weight loss was higher than that of PC@PE, which corresponded to the decomposition of NCC and the loss of the crystal water in LiTFSI. The decomposition of the main chain of PE occurred at 450 °C.

The thermal stability data of the separator is shown in Table 1. T_5 and T_{10} represent the temperature at which the weight loss of separator is 5% and 10%, respectively. The Janus composite separator obtained by the phase inversion had higher T_5 and T_{10} than PE. T_5 of PCP@PE reached 435 °C, which means it had better thermal stability than PE, and fully meets the requirements of battery separator. This was due to the high thermal stability of PEEKK and PAF [7,11].

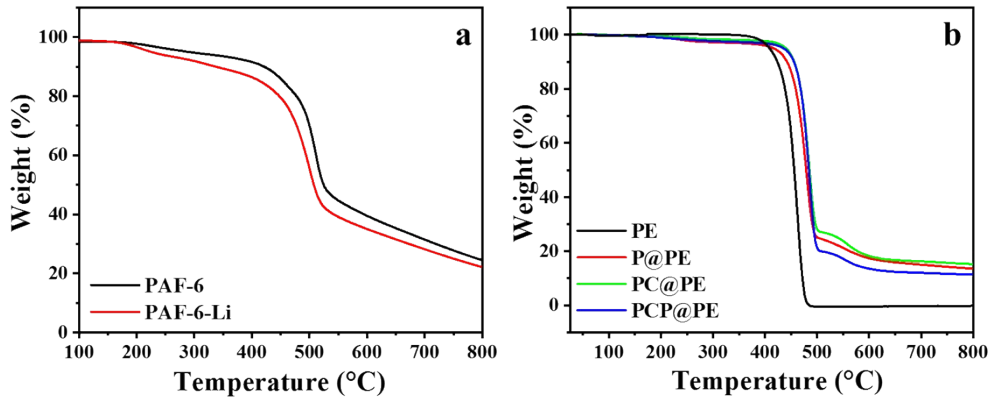

Figure S2. TGA curve of (a) PAF-6, PAF-6-Li recorded in N_2; (b) PE, P@PE, PC@PE, PCP@PE recorded in N_2.

Mechanical Properties

The tensile strength and Young's modulus of the composite separator are shown in Figure S3. The tensile strength of PE was 140 MPa, and the Young's modulus was 550 MPa. P@PE and PC@PE exhibited slightly lower mechanical strength than PE, which should be due to the corrosion of sulfuric acid to PE during the preparation process. The mechanical strength of PCP@PE was higher than that of PE. It shows that

the interface interaction was enhanced due to the hydrogen bonding interaction between PAF-6-Li and the sulfonic acid group on the surface of SPEEKK, thereby improving the mechanical strength of the composite separator with rigid PAF-6-Li [12].

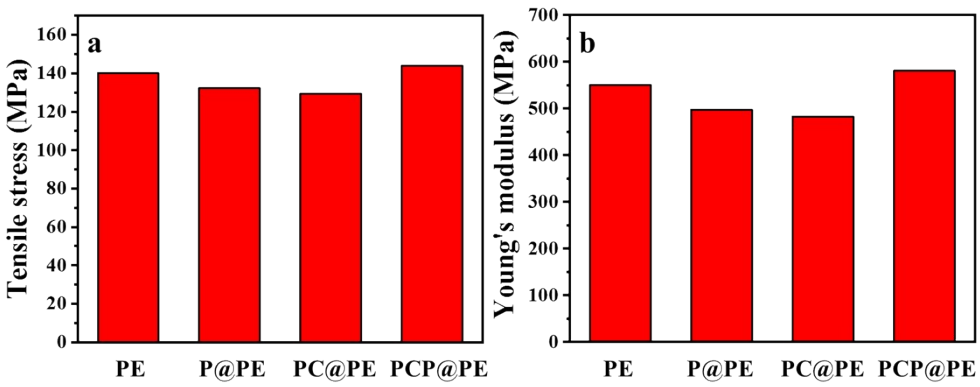

Figure S3. Tensile strength (a) and Young's modulus (b) of composite membranes.

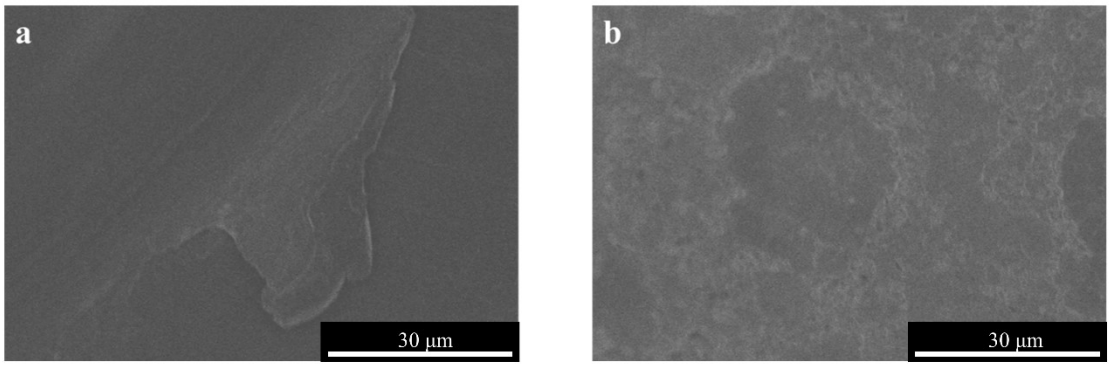

Figure S4. SEM image of the surface topography of (a) Unused Li metal sheet; (b) Li-S battery assembled with the separator of PCP5.0@PE after 200 h cycling under 0.2 C.

SEM image of PE

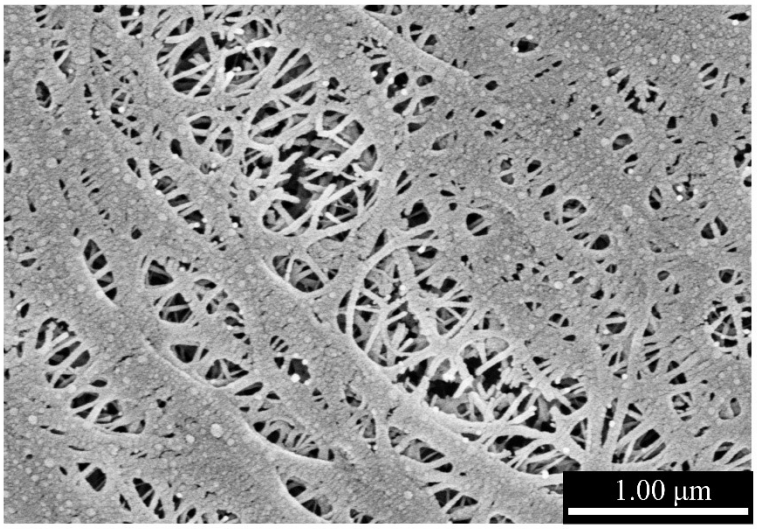

Figure S5. SEM image of PE.

Preparation of Li_2S_6 Solution for Diffusion Experiment:

The synthesis of Li_2S_6 Solution and the operation of the Separator penetration test were similar to those in Ref. S19 and S20, which we referenced and improved upon. S and Li_2S were dissolved in DOL:DME 1:1 (v:v) with a molar ratio of 5:1 to prepare the Li_2S_6 solution with a concentration of 0.5 m. The solution was stirred for 24 h at 60 °C. H-type cells were used to intuitively observe the suppressing effect of two separators on polysulfide. Add 15 mL of Li_2S_6 solution and 15 mL of pure electrolyte solution (DOL:DME 1:1 v:v) to the left and right sides of the H-type cells, separated by a separator in the middle.

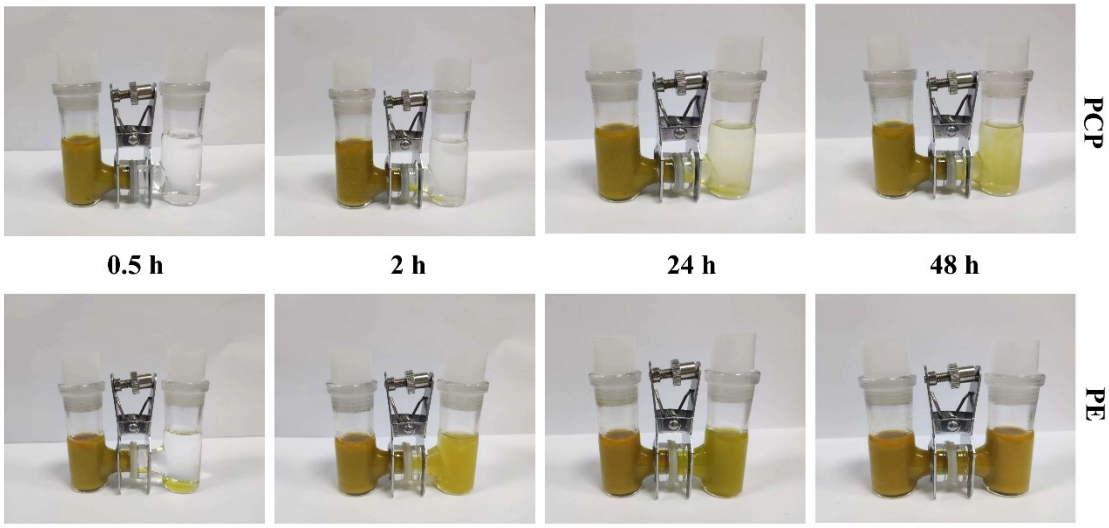

Figure S6. LiPS diffusion in H-type cells with PCP@PE and PE separators.

Table S1. The content of S and Li in the cathode and separator, respectively.

Samples	S 2p (%)	Li 1s (%)
Cathode before cycling	1.24	0
Cathode after cycling	9.01	15.23
Separator before cycling	10.92	4.94
Separator after cycling	15.80	9.80

Table S2. Performance comparison as modified separator applied in Li-S batteries.

Sample	mass loading (mg cm^{-2})	E/S ratio (μL/mg)	Cycling Rate (C)	Intial Capacity (mAh/g)	Cycle number	Residual reversible capacity (mAh/g)	Ref.
Bi_2S_3/rGO	0.2	26.6	0.5	956.0	300	605.0	S13
Ce-	0.28	11.4	0.5	891.0	300	627.0	S14

MOF/Super P							
D-VS_2	0.5	-	0.2	1385.1	200	777.7	S15
RGO@MOS_2	0.24	27.8	0.2	1121.0	200	671.0	S16
Carbon soot	0.15	-	0.2	901.3	100	522.1	S17
COF-CNT	-	-	0.2	1130.0	100	983.1	S18
PCP	0.15	20.8	0.2	1204.0	100	1023.0	This work

References

[S1] Y. Wei, X. Li, Q. Hu, C. Ni, B. Liu, M. Zhang, W. Hu, Sulfonated nanocrystal cellulose/sulfophenylated poly (ether ether ketone ketone) composites for proton exchange membranes, *RSC Adv*. 2016, **6**, 65072-65080.

[S2] H. Zhao, Z. Jin, H. Su, X. Jing, F. Sun, G. Zhu, Targeted synthesis of a 2D ordered porous organic framework for drug release, *Chem. Commun*. 2011, **47**, 6389-6391.

[S3] A. E. Vilian, P. Puthiaraj, C. H. Kwak, S. K. Hwang, Y. S. Huh, W. S. Ahn, Y. K. Han, Fabrication of palladium nanoparticles on porous aromatic frameworks as a sensing platform to detect vanillin, *ACS Appl. Mater. Interfaces* 2016, **8**, 12740-12747.

[S4] W. Lu, D. Yuan, J. Sculley, D. Zhao, H. C. Zhou, Sulfonate-grafted porous polymer networks for preferential CO(2) adsorption at low pressure, *J. Am. Chem. Soc*. 2011, **133**, 18126-18129.

[S5] S. Suriyakumar, A. M. Stephan, N. Angulakshmi, M. H. Hassan, M. H. Alkordi, Metal–organic framework@SiO2 as permselective separator for lithium–sulfur batteries, *J. Mater. Chem. A* 2018, **6**, 14623-14632.

[S6] H. Hareendrakrishnakumar, R. Chulliyote, M. G. Joseph, S. Suriyakumar, A. M. Stephan, Sulfonic groups stemmed ionic shield for polysulfides towards high performance Li–S batteries, *Electrochim. Acta* 2019, **321**, 134697.

[S7] X. Sun, J. H. Song, H. Q. Ren, X. Y. Liu, X. W. Qu, Y. Feng, H. L. Ding, Phosphoric acid-loaded covalent triazine framework for enhanced the proton conductivity of the proton exchange membrane, *Electrochim. Acta* 2020, **331**, 135235.

[S8] S. Ramesh, H. M. Ng, An investigation on PAN–PVC–LiTFSI based polymer electrolytes system, *Solid State Ion*. 2011, **192**, 2-5.

[S9] S. Ramesh, K. C. Wong, Conductivity, dielectric behaviour and thermal stability studies of lithium ion dissociation in poly (methyl methacrylate)-based gel polymer electrolytes, *Ionics* 2009, **15**, 249-254.

[S10] S. Naduparambath, E. Purushothaman, Sago seed shell: determination of the composition and isolation of microcrystalline cellulose (MCC), *Cellulose* 2016, **23**, 1803-1812.

[S11] Y. Gao, G. P. Robertson, M. D. Guiver, S. D. Mikhailenko, X. Li, S. Kaliaguine, Synthesis of copoly (aryl ether ether nitrile) s containing sulfonic acid groups for PEM application, *Macromolecules 2005*, **38**, 3237-3245.

[S12] J. Kung, Superiority and failure mode of automotive batteries insulated with polyethylene separators, *J. Power Sources* 1994, **48**, 129-134.

[S13] L. Zhan, X. Ning, X. Zhou, J. Luo and X. Fan, *Advanced Powder Technology*, 2022, **33**

[S14] Y. Su, W. Wang, W. Wang, A. Wang, Y. Huang and Y. Guan, *Journal of The Electrochemical Society*, 2022, **169**.

[S15] G. Liu, Q. Zeng, Z. Fan, S. Tian, X. Li, X. Lv, W. Zhang, K. Tao, E. Xie and Z. Zhang, *Chemical Engineering Journal*, 2022, **448**.

[S16] L. Tan, X. Li, Z. Wang, H. Guo and J. Wang, *ACS Appl Mater Interfaces*, 2018, **10**, 3707-3713.

[S17] Y. Zhu, J. Wang, Y. Wang, Y. Zhu, Y. Li and S. Zhao, *Ionics*, 2022, **28**, 1693-1700.

[S18] J. Yoo, S. J. Cho, G. Y. Jung, S. H. Kim, K. H. Choi, J. H. Kim, C. K. Lee, S. K. Kwak and S. Y. Lee, *Nano Lett*, 2016, **16**, 3292-3300.

[S19] F. Zhang, X. Guo, P. Xiong, J. Zhang, J. Song, K. Yan, X. Gao, H. Liu and G. Wang, *Advanced Energy Materials*, 2020, **10**.

[S20] J. Li, H. Zhang, L. Luo, H. Li, J. He, H. Zu, L. Liu, H. Liu, F. Wang and J. Song, *Journal of Materials Chemistry A*, 2021, **9**, 2205-2213.